



HAL
open science

Multi-objective Grid-based Lipschitz NLPV PI Observer for Damper Fault Estimation

Gia Quoc Bao Tran, Thanh-Phong Pham, Olivier Sename

► **To cite this version:**

Gia Quoc Bao Tran, Thanh-Phong Pham, Olivier Sename. Multi-objective Grid-based Lipschitz NLPV PI Observer for Damper Fault Estimation. SAFEPROCESS 2022 - 11th IFAC Symposium on Fault Detection, Supervision and Safety for Technical Processes, Jun 2022, Pafos, Cyprus. 10.1016/j.ifacol.2022.07.123 . hal-03611561

HAL Id: hal-03611561

<https://hal.science/hal-03611561>

Submitted on 17 Mar 2022

HAL is a multi-disciplinary open access archive for the deposit and dissemination of scientific research documents, whether they are published or not. The documents may come from teaching and research institutions in France or abroad, or from public or private research centers.

L'archive ouverte pluridisciplinaire **HAL**, est destinée au dépôt et à la diffusion de documents scientifiques de niveau recherche, publiés ou non, émanant des établissements d'enseignement et de recherche français ou étrangers, des laboratoires publics ou privés.

Multi-objective Grid-based Lipschitz NLPV PI Observer for Damper Fault Estimation

Gia Quoc Bao Tran^{*,**} Thanh-Phong Pham^{***}
Olivier Sename^{*}

^{*} Univ. Grenoble Alpes, CNRS, Grenoble INP¹, GIPSA-Lab, 38000 Grenoble, France (¹Institute of Engineering Univ. Grenoble Alpes)
(e-mail: gia-quoc-bao.tran@ieee.org,olivier.sename@grenoble-inp.fr).

^{**} Centre Automatique et Systèmes (CAS),
Mines Paris, Université PSL, 75006 Paris, France.

^{***} Faculty of Electrical and Electronic Engineering, The University of Danang – University of Technology and Education, Danang, Vietnam
(e-mail: ptphong@ute.udn.vn).

Abstract: Dampers in semi-active suspension systems may be subject to various types of damper faults, e.g., oil leakage and electrical issues, that need to be estimated for diagnosis and isolation purposes. A new method to design the so-called multi-objective grid-based Lipschitz Nonlinear Parameter Varying (NLPV) Proportional Integral (PI) observer is here developed for damper fault estimation, where the fault is the loss of efficiency of the damper modeled as a slow-varying input. While the damper nonlinearity is bounded by the Lipschitz condition, the \mathcal{H}_∞ and generalized \mathcal{H}_2 conditions are used to minimize the effects of the input disturbance and the measurement noise, respectively, on the estimation error. Moreover, the observer is designed with Linear Matrix Inequalities (LMIs) formed and solved in a grid-based manner (considering a parameter-dependent Lyapunov function) to reduce the level of conservatism. Analyses in the frequency domain using Bode plots as well as in the time domain using realistic simulations illustrate the effectiveness of the proposed observer.

Keywords: PI observer, Nonlinear Parameter Varying (NLPV), gridding, fault estimation, semi-active suspension.

1. INTRODUCTION

In vehicles, the suspension system is a core part connecting the wheel and the chassis, serving both road holding and driving comfort enhancing purposes by mitigating the excitations transmitted from the road to the chassis where passengers sit (Savaresi et al., 2010; Poussot-Vassal et al., 2012). Among the different types of suspensions (passive, semi-active, and active), the semi-active (SA) one is widely studied and applied since it provides an efficient trade-off between performance and energy consumption (Poussot-Vassal et al., 2012). More particularly, in Electro-Rheological (ER) suspensions considered in this study, an electric field, driven by an applied voltage signal, adjusts the viscosity of the ER fluid in the damper's chamber, thus controlling the damper force. However, this system could be subject to various types of faults (Hernández-Alcántara et al., 2016; Morato et al., 2020), as from the most to the least common, oil leakage (the loss of oil from the damper cylinder), electrical issues in the circuit providing the electric/magnetic field to drive the damper, and physical deformation of the cylinder. These faults lead to the loss of damper efficiency; therefore, fault diagnosis and estimation are indeed crucial issues for reliability.

Many studies have been conducted on fault detection and estimation in various systems. In particular, several fault

estimation filters are proposed in (Varga and Ossmann, 2014; Vanek et al., 2014; Rodrigues et al., 2013; Chen et al., 2016) with applications mainly in transports and machines. Among all possible methods, the Proportional Integral (PI) observer is of high interest given that the fault is slow-varying and can then be modeled as an additional state (Do et al., 2018; Guzman et al., 2021). Such a method has been considered for input estimation purposes, such as in (Yamamoto et al., 2019) for driver torque estimation in electric power steering. However, while several methods do exist for damper force (not fault) estimation (Pham et al., 2019; Pham et al., 2019; Do et al., 2020; Tran et al., 2021), and more recently (Pham et al., 2021) with a nonlinear observer or (Tudon-Martinez et al., 2021) with a Linear Parameter Varying (LPV) filter, only few do tackle the fault estimation problem. Let us cite (Morato et al., 2019) where an LPV polytopic fault detection observer has been proposed.

In this paper, we consider the problem of estimating slow-varying additive faults in dampers, where the lost damper force is modeled as an external input. Our objective is fault estimation using a Nonlinear Parameter Varying (NLPV) PI observer, with the following contributions:

- The only assumption on the fault dynamics (which should be unknown) is that it is slow-varying, which is the most basic one so as not to narrow the scope

of this study. This assumption can be justified for the considered kind of fault (damper loss of efficiency), which is not abrupt faults;

- The only considered measurements are accelerations of the sprung and unsprung masses measured using accelerometers, which have advantages over deflection sensors, e.g., low cost and ease of installation;
- A new method to handle the damper nonlinearity is proposed. Indeed, since the PWM control input is actually known and bounded in practice, considering the nonlinear dynamics of the damper force's controlled part as seen later in (2) is more realistic than bounding and calculating the force as a scheduling parameter as in (Morato et al., 2019). Moreover, the influence of the system's nonlinearity on the estimation error is bounded by the Lipschitz condition, thus decreasing the level of conservatism compared to (Tran et al., 2021) where that disturbance is merely considered bounded by a given constant;
- The \mathcal{H}_∞ and generalized \mathcal{H}_2 ($g\mathcal{H}_2$) conditions are used to bound the effects of the input disturbance and the measurement noise, respectively, on the estimation error. Indeed, the former minimizes the effects of the disturbance in the whole frequency range, while the latter is more suited for handling white noise coming from sensors (Tran et al., 2021). Besides, speeding up convergence via pole placement is necessary in PI observers. The \mathcal{S} -procedure (Boyd et al., 1994) is used to combine all said objectives into a single framework;
- The grid-based method is considered here for LMI solving and gain scheduling, where the perfectly known scheduling parameter is the PWM control input. Compared to the polytopic approach, gridding is less conservative, thanks to the use of a parameter-dependent Lyapunov function (associated with robust stability) rather than a constant one (associated with quadratic stability that is harder to satisfy).

This paper is organized as follows. In Section 2, the considered system and the associated model are presented. In Section 3, the observer design problem is described and solved. The synthesis results and analyses are presented in Section 4. Some realistic simulation results are detailed in Section 5. Finally, the conclusion is drawn in Section 6.

2. SYSTEM DESCRIPTION AND MODELING

2.1 The Semi-active Suspension

The suspension system is studied by considering the quarter-car model consisting of the sprung and unsprung masses (m_s and m_{us}) as illustrated in Figure 1 (Savaresi et al., 2010). Applying Newton's law of motion, we obtain

$$\begin{cases} m_s \ddot{z}_s = -F_s - F_d \\ m_{us} \ddot{z}_{us} = F_s + F_d - F_t. \end{cases} \quad (1)$$

The spring force is $F_s = k_s z_{def}$ where $z_{def} = z_s - z_{us}$ is the suspension deflection and \dot{z}_{def} the deflection velocity; the tire force is $F_t = k_t(z_{us} - z_r)$. The dynamics of the damper force F_d are expressed as (Pham et al., 2019)

$$\begin{cases} F_d = \underbrace{k_0 z_{def} + c_0 \dot{z}_{def}}_{F_{passive}} + F_{er} \\ \dot{F}_{er} = \frac{-1}{\tau} F_{er} + \frac{f_c}{\tau} \cdot u \cdot \tanh(k_1 z_{def} + c_1 \dot{z}_{def}), \end{cases} \quad (2)$$

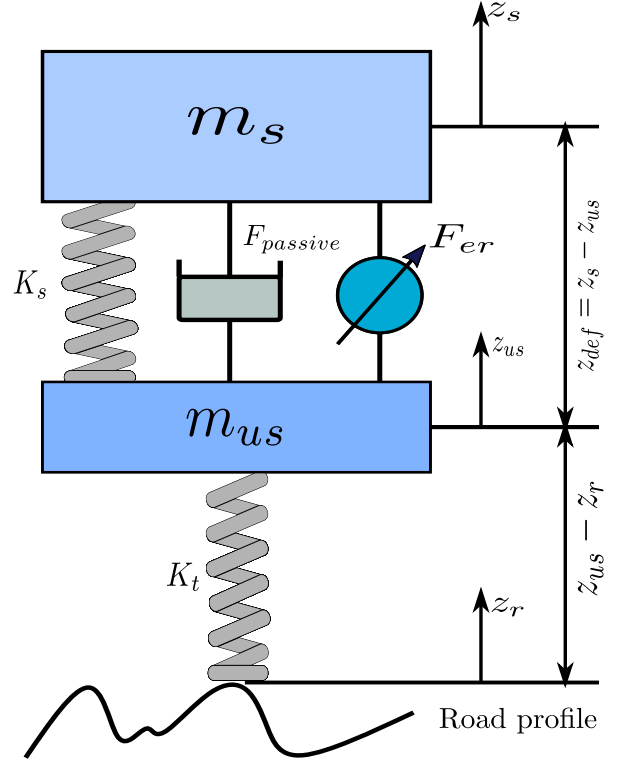


Fig. 1. The quarter-car model.

where F_{er} is the controlled part of the damper force; c_0 , c_1 , k_0 , k_1 , f_c , and τ are constant parameters; $u \in [0, 1]$ is the duty cycle of the PWM control input signal.

2.2 Faulty System Modeling

Consider now that the ER damper is subject to one of the two most common types of fault which are oil leakage from the cylinder and electrical issues (Morato et al., 2020). Any of these faults will lead to a loss in the damper force. As a result, the faulty damper force is written as

$$F_f = F_d - f, \quad (3)$$

where f is the damper fault (representing a loss of force). The objective of this paper is to estimate the additive fault f in the presence of unknown inputs (with the damper force either known or independently estimated as a linear combination of the states (Tran et al., 2021)).

Defining the state as $x = (z_s - z_{us} \quad \dot{z}_s \quad z_{us} - z_r \quad \dot{z}_{us} \quad F_{er})^\top$, we can write the system in (1)-(2)-(3) as the following NLPV state-space representation (Pham et al., 2021)

$$\Sigma(\rho) : \begin{cases} \dot{x} = Ax + B(\rho)\Phi(x) + E_1 f + D_1 \omega_r \\ y = Cx + E_2 f + D_2 \omega_n, \end{cases} \quad (4)$$

where the measured output vector y is $(\ddot{z}_s \quad \ddot{z}_{us})^\top \in \mathbb{R}^2$ (accelerations) assuming some measurement noises ω_n ; the input disturbance is $\omega_r = \dot{z}_r$. The known scheduling parameter is $\rho = u \in [\underline{\rho}, \bar{\rho}]$ (the minimum and maximum PWM values). In (4), $\Phi(x) = \tanh(k_1 z_{def} + c_1 \dot{z}_{def}) := \tanh(\Gamma x)$ with $\Gamma = (k_1 \quad c_1 \quad 0 \quad -c_1 \quad 0)$. Note that $\Phi(x)$ is Lipschitz, i.e.,

$$\|\Phi(x) - \Phi(\hat{x})\| \leq \|\Gamma(x - \hat{x})\|, \forall x, \hat{x}. \quad (5)$$

The faulty system matrices are (with $k = k_s + k_0$):

$$A = \begin{pmatrix} 0 & 1 & 0 & -1 & 0 \\ -k & -c_0 & 0 & c_0 & -1 \\ m_s & m_s & 0 & m_s & m_s \\ 0 & 0 & 0 & 1 & 0 \\ k & c_0 & -k_t & -c_0 & 1 \\ m_{us} & m_{us} & m_{us} & m_{us} & \frac{m_{us}}{\tau} \\ 0 & 0 & 0 & 0 & \frac{1}{\tau} \end{pmatrix}, B(\rho) = \begin{pmatrix} 0 \\ 0 \\ 0 \\ 0 \\ f_c \frac{\rho}{\tau} \end{pmatrix}, E_1 = \begin{pmatrix} 0 \\ 1 \\ m_s \\ 0 \\ -1 \\ m_{us} \\ 0 \end{pmatrix},$$

$$E_2 = \begin{pmatrix} 1 \\ m_s \\ -1 \\ m_{us} \end{pmatrix}, D_1 = \begin{pmatrix} 0 \\ 0 \\ -1 \\ 0 \\ 0 \end{pmatrix}, C = \begin{pmatrix} -k & k \\ m_s & m_{us} \\ -c_0 & c_0 \\ m_s & m_{us} \\ 0 & -k_t \\ c_0 & -c_0 \\ m_s & m_{us} \\ -1 & 1 \\ m_s & m_{us} \end{pmatrix}^\top, D_2 = \begin{pmatrix} 10^{-2} \\ 10^{-3} \end{pmatrix}.$$

In this work, the model parameter values used for simulations are those in (Pham et al., 2019).

3. OBSERVER DESIGN METHOD

In this Section, the observer design problem is formulated and the design method is detailed.

3.1 Problem Formulation

Consider the NLPV system (4). Let us suppose the lack of knowledge on the dynamics of the fault. Assumption 1 is thus made, which is standard in fault or input estimation methods such as (Morato et al., 2019; Yamamoto et al., 2015).

Assumption 1. The fault is slow-varying, i.e., $\dot{f} \simeq 0$.

Following Assumption 1, denoting the extended state as $x_e = (x \ f)^\top$, we derive the extended NLPV state-space representation as

$$\begin{cases} \dot{x}_e = A_e x_e + B_e(\rho)\Phi(x) + D_{1e}\omega_r \\ y = C_e x_e + D_2\omega_n, \end{cases} \quad (6)$$

where $A_e = \begin{pmatrix} A & E_1 \\ 0 & 0 \end{pmatrix}$, $B_e(\rho) = \begin{pmatrix} B(\rho) \\ 0 \end{pmatrix}$, $D_{1e} = \begin{pmatrix} D_1 \\ 0 \end{pmatrix}$, and $C_e = (C \ E_2)$.

Let us consider the NLPV PI observer

$$\mathcal{O}(\rho) : \begin{cases} \dot{\hat{x}} = A\hat{x} + B(\rho)\Phi(\hat{x}) + E_1\hat{f} + L_p(\rho)(y - C_e\hat{x}_e) \\ \dot{\hat{f}} = L_i(\rho)(y - C_e\hat{x}_e), \end{cases} \quad (7)$$

where \hat{x} and \hat{f} are the estimates of x and f . Denote $e = x_e - \hat{x}_e$ (where $\hat{x}_e = (\hat{x} \ \hat{f})^\top$) as the estimation error where \hat{x}_e is the estimate of x_e and $e_f = f - \hat{f}$ as the estimation output. We denote also $x - \hat{x} = C_x e$ where $C_x = (I \ 0_{5 \times 1})$. Subtracting (7) from (4) and using (6), we obtain the error system

$$\begin{cases} \dot{e} = (A_e - L(\rho)C_e)e + B_e(\rho)\Delta\Phi + D_{1e}\omega_r - L(\rho)D_2\omega_n \\ e_f = C_f e, \end{cases} \quad (8)$$

where $\Delta\Phi = \Phi(x) - \Phi(\hat{x})$ satisfies (5), $L(\rho) = (L_p(\rho) \ L_i(\rho))^\top$ is the observer gain to be found, and $C_f = (0_{1 \times 5} \ 1)$.

While the term $\Delta\Phi$ is bounded by the Lipschitz condition (5), the multi-objective $(\mathcal{H}_\infty/g\mathcal{H}_2)$ NLPV PI observer design problem is to find $L(\rho)$ such that

- The error system (8) is asymptotically stable for $\omega_r(t) = 0$ and $\omega_n(t) = 0$;
- $\|e_f(t)\|_2 < \gamma_\infty \|\omega_r(t)\|_2$ for $\omega_r(t) \neq 0$ and $\|e_f(t)\|_\infty < \gamma_2 \|\omega_n(t)\|_2$ for $\omega_n(t) \neq 0$;
- The poles of the system (8) are sufficiently fast to ensure the time-domain efficiency of the observer.

The multi-objective problem will be solved considering the combined performance index $\alpha\gamma_\infty + (1 - \alpha)\gamma_2$ to be minimized given $\alpha \in [0, 1]$. Note that when (8) is asymptotically stable, the error e tends to 0 since $\Delta\Phi$ vanishes as \hat{x} approaches x . Note also that the $g\mathcal{H}_2$ condition is used here for the noise attenuation objective.

3.2 Grid-based Design of the NLPV PI Observer

A parameter-dependent Lyapunov function is considered here to tackle the stability proof of the estimation error; therefore, the following assumption is needed for the scheduling parameter derivative.

Assumption 2. The scheduling parameter's derivative is bounded, i.e., $|\dot{\rho}| \leq \nu$.

The observer is then designed using Theorem 1.

Theorem 1. Under Assumption 2, the observer design problem is solved if, given a constant $\alpha \in [0, 1]$ and a decay rate constraint $\beta \geq 0$, there exist $X(\rho) = X^\top(\rho) > 0$, $Y(\rho)$, and $\epsilon_l > 0$ minimizing $\alpha\gamma_\infty + (1 - \alpha)\gamma_2$ and satisfying for all ρ , the set of LMIs

$$\begin{pmatrix} \Omega(\rho) + C_f^\top C_f & X(\rho)B_e(\rho) & X(\rho)D_{1e} \\ B_e^\top(\rho)X(\rho) & -\epsilon_l I & 0 \\ D_{1e}^\top X(\rho) & 0 & -\gamma_\infty^2 I \end{pmatrix} < 0, \quad (9)$$

$$\begin{pmatrix} \Omega(\rho) & X(\rho)B_e(\rho) & Y(\rho)D_2 \\ B_e^\top(\rho)X(\rho) & -\epsilon_l I & 0 \\ D_2^\top Y^\top(\rho) & 0 & -I \end{pmatrix} < 0,$$

$$\begin{pmatrix} X(\rho) & C_f^\top \\ C_f & \gamma_2^2 I \end{pmatrix} > 0,$$

where $\Omega(\rho) = A_e^\top X(\rho) + X(\rho)A_e + C_e^\top Y^\top(\rho) + Y(\rho)C_e \pm \nu \frac{\partial X(\rho)}{\partial \rho} + 2\beta X(\rho) + \epsilon_l C_x^\top \Gamma^\top \Gamma C_x$. Then, the observer gain is found as $L(\rho) = -X^{-1}(\rho)Y(\rho)$.

Note that the decay rate constraint with β is used here to enhance the dynamical performances of the estimation.

Proof 1. Consider the parameter-dependent Lyapunov function candidate $V(e, \rho) = e^\top X(\rho)e$ where $X(\rho) = X^\top(\rho) > 0$. Denote $\eta_1 = (e \ \Delta\Phi \ \omega_r)^\top$ and $\eta_2 = (e \ \Delta\Phi \ \omega_n)^\top$. Choosing a decay rate bound of β for the error e , we derive

$$\begin{aligned} & \dot{V}(e, \rho) + 2\beta V(e, \rho) \\ &= \dot{e}^\top X(\rho)e + e^\top X(\rho)\dot{e} + e^\top \left(\dot{\rho} \frac{\partial X(\rho)}{\partial \rho} \right) e + 2\beta e^\top X(\rho)e \\ &= e^\top \left[(A_e - L(\rho)C_e)^\top X(\rho) + X(\rho)(A_e - L(\rho)C_e) \right. \\ & \quad \left. + \dot{\rho} \frac{\partial X(\rho)}{\partial \rho} + 2\beta X(\rho) \right] e + e^\top X(\rho)B_e(\rho)\Delta\Phi \\ & \quad + \Delta\Phi^\top B_e^\top(\rho)X(\rho)e + e^\top X(\rho)D_{1e}\omega_r + \omega_r^\top D_{1e}^\top X(\rho)e \\ & \quad - e^\top X(\rho)L(\rho)D_2\omega_n - \omega_n^\top D_2^\top L^\top(\rho)X(\rho)e. \end{aligned} \quad (10)$$

Here, we consider ω_r and ω_n as unknown external inputs. Using the superposition theorem and introducing the variable $Y(\rho) = -X(\rho)L(\rho)$, we consider first $\omega_n = 0$ and then $\omega_r = 0$, and separate the \mathcal{H}_∞ and $g\mathcal{H}_2$ problems as

$$\begin{aligned}
& \dot{V}_1(e, \rho) \\
&= e^\top \left[(A_e - L(\rho)C_e)^\top X(\rho) + X(\rho)(A_e - L(\rho)C_e)(\rho) \right. \\
&+ \dot{\rho} \frac{\partial X(\rho)}{\partial \rho} + 2\beta X(\rho) \left. \right] e + e^\top X(\rho) B_e(\rho) \Delta \Phi \\
&+ \Delta \Phi^\top B_e^\top(\rho) X(\rho) e + e^\top X(\rho) D_{1e} \omega_r + \omega_r^\top D_{1e}^\top X(\rho) e \\
&= \eta_1^\top \underbrace{\begin{pmatrix} \Omega_1(\rho) & X(\rho) B_e(\rho) & X(\rho) D_{1e} \\ B_e^\top(\rho) X(\rho) & 0 & 0 \\ D_{1e}^\top X(\rho) & 0 & 0 \end{pmatrix}}_{\mathcal{Q}_1(\rho)} \eta_1,
\end{aligned}$$

$$\begin{aligned}
& \dot{V}_2(e, \rho) \\
&= e^\top \left[(A_e - L(\rho)C_e)^\top X(\rho) + X(\rho)(A_e - L(\rho)C_e)(\rho) \right. \\
&+ \dot{\rho} \frac{\partial X(\rho)}{\partial \rho} + 2\beta X(\rho) \left. \right] e + e^\top X(\rho) B_e(\rho) \Delta \Phi \\
&+ \Delta \Phi^\top B_e^\top(\rho) X(\rho) e + e^\top Y(\rho) D_2 \omega_n + \omega_n^\top D_2^\top Y^\top(\rho) e \\
&= \eta_2^\top \underbrace{\begin{pmatrix} \Omega_1(\rho) & X(\rho) B_e(\rho) & Y(\rho) D_2 \\ B_e^\top(\rho) X(\rho) & 0 & 0 \\ D_2^\top Y^\top(\rho) & 0 & 0 \end{pmatrix}}_{\mathcal{Q}_2(\rho)} \eta_2,
\end{aligned} \tag{11}$$

where $\Omega_1(\rho) = A_e^\top X(\rho) + X(\rho) A_e + C_e^\top Y^\top(\rho) + Y(\rho) C_e + \dot{\rho} \frac{\partial X(\rho)}{\partial \rho} + 2\beta X(\rho)$. Then, the Lipschitz condition (5) gives

$$\Delta \Phi^\top \Delta \Phi \leq e^\top C_x^\top \Gamma^\top \Gamma C_x e.$$

This condition (independent of ω_r and ω_n) is rewritten as

$$\eta_1^\top \mathcal{Q}_3 \eta_1 \leq 0, \quad \eta_2^\top \mathcal{Q}_3 \eta_2 \leq 0, \tag{12}$$

where $\mathcal{Q}_3 = \begin{pmatrix} -C_x^\top \Gamma^\top \Gamma C_x & 0 & 0 \\ 0 & I & 0 \\ 0 & 0 & 0 \end{pmatrix}$. Next, let us define the following terms

$$J_1 = e_f^\top e_f - \gamma_\infty^2 \omega_r^\top \omega_r = \eta_1^\top \underbrace{\begin{pmatrix} C_f^\top C_f & 0 & 0 \\ 0 & 0 & 0 \\ 0 & 0 & -\gamma_\infty^2 I \end{pmatrix}}_{\mathcal{Q}_4} \eta_1,$$

$$J_2 = -\omega_n^\top \omega_n = \eta_2^\top \begin{pmatrix} 0 & 0 & 0 \\ 0 & 0 & 0 \\ 0 & 0 & -I \end{pmatrix} \eta_2 := \eta_2^\top \mathcal{Q}_5 \eta_2,$$

$$J_3(\rho) = \gamma_2^2 e^\top X(\rho) e - e_f^\top e_f = e^\top \underbrace{(\gamma_2^2 X(\rho) - C_f^\top C_f)}_{\mathcal{Q}_6(\rho)} e.$$

The \mathcal{H}_∞ and $g\mathcal{H}_2$ conditions give (as (8) is strictly proper)

$$\begin{cases} \dot{V}_1(e, \rho) + J_1 < 0 \\ \dot{V}_2(e, \rho) + J_2 < 0 \\ J_3(\rho) > 0. \end{cases} \tag{13}$$

When the \mathcal{S} -procedure (Boyd et al., 1994) is applied to the constraints (12) and conditions (13), $\dot{V}_1(e, \rho) < 0$ and $\dot{V}_2(e, \rho) < 0$ if there exists a scalar $\epsilon_l > 0$ s.t.

$$\begin{aligned}
& \begin{cases} \dot{V}_1(e, \rho) - \epsilon_l \eta_1^\top \mathcal{Q}_3 \eta_1 + J_1 < 0 \\ \dot{V}_2(e, \rho) - \epsilon_l \eta_2^\top \mathcal{Q}_3 \eta_2 + J_2 < 0 \\ J_3(\rho) > 0 \end{cases} \\
& \iff \begin{cases} \eta_1^\top (\mathcal{Q}_1(\rho) - \epsilon_l \mathcal{Q}_3 + \mathcal{Q}_4) \eta_1 < 0 \\ \eta_2^\top (\mathcal{Q}_2(\rho) - \epsilon_l \mathcal{Q}_3 + \mathcal{Q}_5) \eta_2 < 0 \\ e^\top \mathcal{Q}_6(\rho) e > 0 \end{cases} \\
& \iff \begin{cases} \mathcal{Q}_1(\rho) - \epsilon_l \mathcal{Q}_3 + \mathcal{Q}_4 < 0 \\ \mathcal{Q}_2(\rho) - \epsilon_l \mathcal{Q}_3 + \mathcal{Q}_5 < 0 \\ \mathcal{Q}_6(\rho) > 0, \end{cases}
\end{aligned}$$

which is equivalent to

$$\begin{aligned}
& \begin{pmatrix} \Omega_2(\rho) + C_f^\top C_f & X(\rho) B_e(\rho) & X(\rho) D_{1e} \\ B_e^\top(\rho) X(\rho) & -\epsilon_l I & 0 \\ D_{1e}^\top X(\rho) & 0 & -\gamma_\infty^2 I \end{pmatrix} < 0, \\
& \begin{pmatrix} \Omega_2(\rho) & X(\rho) B_e(\rho) & Y(\rho) D_2 \\ B_e^\top(\rho) X(\rho) & -\epsilon_l I & 0 \\ D_2^\top Y^\top(\rho) & 0 & -I \end{pmatrix} < 0, \\
& \gamma_2^2 X(\rho) - C_f^\top C_f > 0,
\end{aligned} \tag{14}$$

where $\Omega_2(\rho) = \Omega_1(\rho) + \epsilon_l C_x^\top \Gamma^\top \Gamma C_x$. Then, Schur's lemma is applied to the third condition in (14). Under Assumption 2, (14) is satisfied if and only if (9) is satisfied (Wu, 1995). Last, (13) ensures the $\mathcal{H}_\infty/g\mathcal{H}_2$ performance:

$$\begin{aligned}
& \|e_f(t)\|_2^2 < \gamma_\infty^2 \|\omega_r(t)\|_2^2, \\
& \|e_f(t)\|_\infty^2 < \gamma_2^2 \|\omega_n(t)\|_2^2.
\end{aligned}$$

The proof is completed. \square

Remark 1. In the case the error system (8) has no external inputs, by guaranteeing $\dot{V}_1(e, \rho) < 0$ and $\dot{V}_2(e, \rho) < 0$, we get $\dot{V}(e, \rho) + 2\beta V(e, \rho) < 0$ for the quadratic Lyapunov function candidate, thus imposing a decay rate of faster than $\frac{1}{\beta}$ (if $\beta > 0$). This use of pole placement to speed up the convergence rate is crucial in PI observers for estimating slow-varying inputs, as seen in (Yamamoto et al., 2015). As $V(e, \rho) > 0$, that implies $\dot{V}(e, \rho) < 0$, which guarantees the asymptotic stability of the error (as $X(\rho)$ has strictly positive bounds with $\rho \in [\underline{\rho}, \bar{\rho}]$).

The LMIs formed in (9) must be satisfied for an infinite number of values of ρ . Therefore, these inequalities are here solved in a grid-based manner (Wu, 1995), i.e., satisfied at a set of frozen values belonging to a gridded domain of ρ , together with Assumption 2. Moreover, since gridding is used here for LMI solving, the asymptotic stability of the error associated with the obtained solution must be re-checked using a much denser grid (Wu, 1995).

4. OBSERVER SYNTHESIS RESULTS

The observer is designed for the suspension considering:

- $X(\rho) = X_0 + \rho X_1$ so $\frac{\partial X(\rho)}{\partial \rho} = X_1$, and $Y(\rho) = Y_0 + \rho Y_1$ (note that more complex forms can indeed be chosen);
- Ten grid points with ρ evenly spaced in $[\underline{\rho}, \bar{\rho}]$ where $\underline{\rho} = 0.1$ and $\bar{\rho} = 0.5$ for safety purposes (recall $\rho = u$);
- $\beta = 8$ for an efficient convergence rate;
- $\nu = 1000 \text{ s}^{-1}$, while $\frac{\bar{\rho} - \underline{\rho}}{T_s} = 80 \text{ s}^{-1}$ with $T_s = 0.005 \text{ s}$ the experiment sampling time (Pham et al., 2019).

With CVX (Grant and Boyd, 2014) and the SDPT3 solver, one obtained solution is such that $\gamma_\infty = 0.9$ and $\gamma_2 = 0.87$.

Remark 2. The fault has been normalized for observer design purposes.

4.1 Analysis of the Unknown Inputs' Effects

To evaluate the influence of unknown inputs, Bode diagrams of the error systems ($\frac{e_f}{\omega_r}$ and $\frac{e_f}{\omega_n}$), frozen at the grid points, are shown in Figure 2. This shows a satisfactory attenuation level of below -65 dB for any input disturbance and -80 dB for the measurement noise in high frequencies.

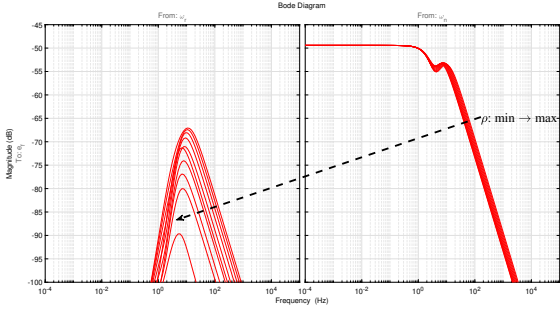


Fig. 2. Bode plots ($\frac{e_f}{w_r}$ and $\frac{e_f}{w_n}$) of the frozen error systems.

4.2 Analysis of the Nonlinearity's Effects

The effects of the disturbance caused by the nonlinearity $\Delta\Phi$ on the error are illustrated in the frozen Bode plots in Figure 3. Attenuation is well achieved, especially in low to middle frequency ranges where this term acts. This emphasizes the interest and efficiency of the proposed NLPV observer design method (handling the nonlinearity through the Lipschitz condition).

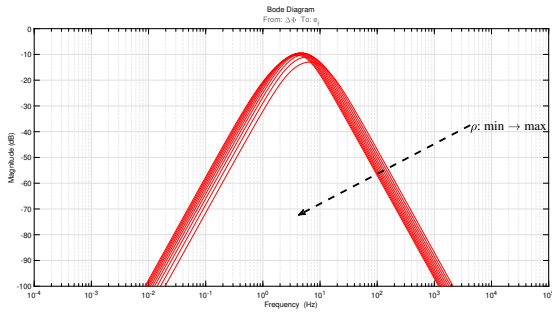


Fig. 3. Bode plots ($\frac{e_f}{\Delta\Phi}$) of the frozen error systems.

5. OBSERVER APPLICATION RESULTS

The observer is implemented as in Figure 4.

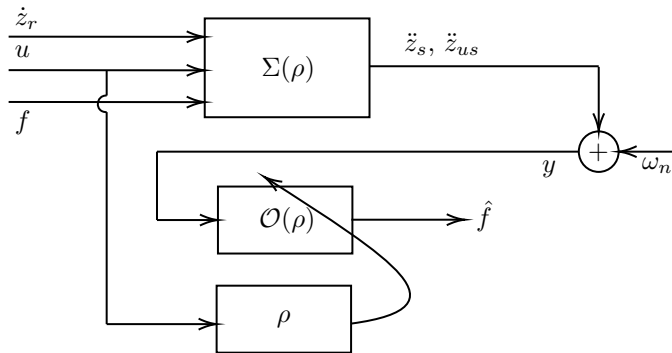


Fig. 4. Implementation of the observer.

5.1 Validation Scheme

Even though the fault (lost damper force) is modeled as an input in order to apply the PI observer, it is not a real input, and hence its variation in time should be similar to

the damper force itself. The way we propose to validate the scheme (either in simulations or experiments) is:

- Conduct one test with a nominal (faultless) case;
- Conduct the faulty case where the fault (lost force) that is a portion of the faultless damper force is subtracted from the damper force.

5.2 Simulation Results

In this simulation scenario lasting 20 seconds, we use:

- An ISO road profile of type C;
- A skyhook controller that gives the PWM signal;
- Measurement noise with zero mean and unit variance.

The road profile is shown in Figure 5.

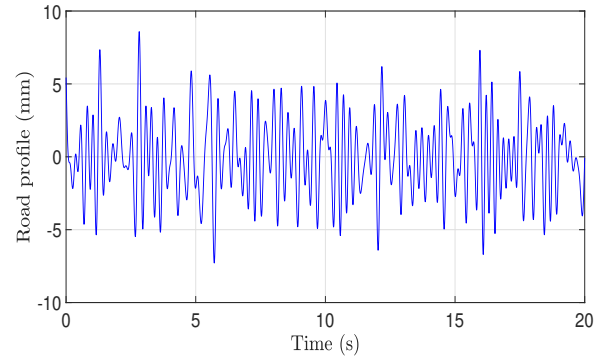


Fig. 5. The road profile used for simulation.

Figure 6 shows the resulting measurements (accelerations).

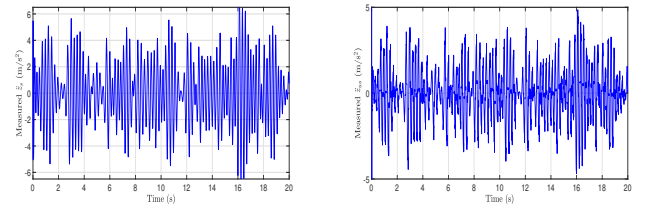


Fig. 6. Measured sprung (left) and unsprung mass accelerations (right).

Fault estimation results are shown in Figure 7. It can be observed that only practical convergence is achieved because Assumption 1 is not strictly respected in practice.

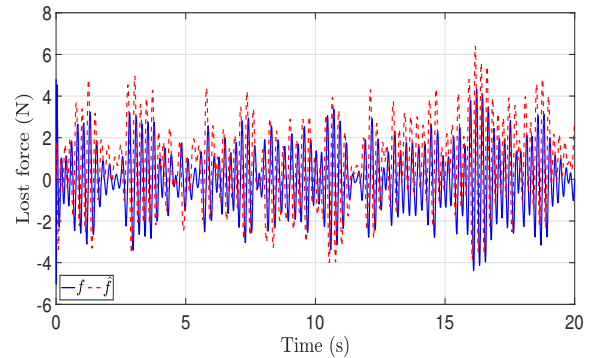


Fig. 7. Estimated lost damper force.

6. CONCLUSION

This paper proposes an NLPV PI observer for fault estimation in the SA suspension, with the most basic assumption on the fault dynamics (slow-varying). This observer is obtained by forming and solving LMIs in a grid-based manner to lower conservatism, where the Lipschitz condition is used to bound the nonlinearity in the system, while the \mathcal{H}_∞ and $g\mathcal{H}_2$ conditions are used to treat the input disturbance and the measurement noise, respectively. Evaluation and analysis in both the frequency domain using Bode plots and the time domain using simulations illustrate the method's effectiveness.

In the future, more advanced fault estimation methods, e.g., the descriptor form observer (which does not require Assumption 1), will be developed based on this work. Experimental validation is currently being investigated.

REFERENCES

- Boyd, S., El Ghaoui, L., Feron, E., and Balakrishnan, V. (1994). *Linear Matrix Inequalities in System and Control Theory*. SIAM.
- Chen, L., Patton, R., and Goupil, P. (2016). Robust Fault Estimation using an LPV Reference Model: ADDSAFE Benchmark Case Study. *Control Engineering Practice*, 49, 194–203. doi: <https://doi.org/10.1016/j.conengprac.2015.12.006>.
- Do, M.H., Koenig, D., and Theilliol, D. (2018). Robust H_∞ Proportional-Integral Observer for Fault Diagnosis: Application to Vehicle Suspension. *IFAC-PapersOnLine*, 51(24), 536–543. doi: <https://doi.org/10.1016/j.ifacol.2018.09.628>. 10th IFAC Symposium on Fault Detection, Supervision and Safety for Technical Processes SAFEPROCESS 2018.
- Do, M.H., Koenig, D., and Theilliol, D. (2020). Robust H_∞ Proportional-integral Observer-based Controller for Uncertain LPV System. *Journal of the Franklin Institute*, 357(4), 2099–2130. doi: <https://doi.org/10.1016/j.jfranklin.2019.11.053>.
- Grant, M. and Boyd, S. (2014). CVX: Matlab Software for Disciplined Convex Programming, version 2.1. <http://cvxr.com/cvx>.
- Guzman, J., López-Estrada, F.R., Estrada-Manzo, V., and Valencia-Palomo, G. (2021). Actuator Fault Estimation based on a Proportional-integral Observer with Non-quadratic Lyapunov Functions. *International Journal of Systems Science*, 1–14.
- Hernández-Alcántara, D., Tudón-Martínez, J.C., Amézquita-Brooks, L., Vivas-López, C.A., and Morales-Menéndez, R. (2016). Modeling, Diagnosis and Estimation of Actuator Faults in Vehicle Suspensions. *Control Engineering Practice*, 49, 173–186. doi: <https://doi.org/10.1016/j.conengprac.2015.12.002>.
- Morato, M.M., Sename, O., Dugard, L., and Nguyen, M.Q. (2019). Fault Estimation for Automotive Electro-Rheological Dampers: LPV-based Observer Approach. *Control Engineering Practice*, 85, 11–22. doi: <https://doi.org/10.1016/j.conengprac.2019.01.005>.
- Morato, M., Pham, T.P., Sename, O., and Dugard, L. (2020). Development of a Simple ER Damper Model for Fault-tolerant Control Design. *Journal of the Brazilian Society of Mechanical Sciences and Engineering*, 42(10), 502 (2020). doi:10.1007/s40430-020-02585-y.
- Pham, T.P., Sename, O., and Dugard, L. (2019). Unified \mathcal{H}_∞ Observer for a Class of Nonlinear Lipschitz Systems: Application to a Real ER Automotive Suspension. *IEEE Control Systems Letters*, 3(4), 817–822. doi: 10.1109/LCSYS.2019.2919813.
- Pham, T.P., Sename, O., and Dugard, L. (2019). Real-time Damper Force Estimation of Vehicle Electrorheological Suspension: A NonLinear Parameter Varying Approach. *IFAC-PapersOnLine*, 52(28), 94–99. doi: <https://doi.org/10.1016/j.ifacol.2019.12.354>. 3rd IFAC Workshop on Linear Parameter Varying Systems 2019.
- Pham, T.P., Sename, O., and Dugard, L. (2021). A Nonlinear Parameter Varying Observer for Real-time Damper Force Estimation of an Automotive Electro-rheological Suspension System. *International Journal of Robust and Nonlinear Control*. doi:10.1002/rnc.5583.
- Poussot-Vassal, C., Spelta, C., Sename, O., Savaresi, S., and Dugard, L. (2012). Survey and Performance Evaluation on Some Automotive Semi-active Suspension Control Methods: A Comparative Study on a Single-corner Model. *Annual Reviews in Control*, 36(1), 148–160. doi: <https://doi.org/10.1016/j.arcontrol.2012.03.011>.
- Rodrigues, M., Sahnoun, M., Theilliol, D., and Ponsart, J.C. (2013). Sensor Fault Detection and Isolation Filter for Polytopic LPV Systems: A Winding Machine Application. *Journal of Process Control*, 23(6), 805–816. doi: <https://doi.org/10.1016/j.jprocont.2013.04.002>.
- Savaresi, S., Poussot-Vassal, C., Spelta, C., Sename, O., and Dugard, L. (2010). *Semi-Active Suspension Control for Vehicles*. Elsevier - Butterworth Heinemann.
- Tran, G.Q.B., Pham, T.P., and Sename, O. (2021). Multi-objective Unified qLPV Observer: Application to a Semi-active Suspension System. *IFAC-PapersOnLine*, 54(8), 136–141. doi: <https://doi.org/10.1016/j.ifacol.2021.08.593>. 4th IFAC Workshop on Linear Parameter Varying Systems.
- Tudon-Martínez, J.C., Amézquita-Brooks, L., Hernández-Alcántara, D., and Sename, O. (2021). Semi Active Damping Force Estimation Using LPV- H_∞ Estimators with Different Sensing Configurations. *Journal of the Franklin Institute*. doi: <https://doi.org/10.1016/j.jfranklin.2021.08.031>.
- Vanek, B., Edelmayer, A., Szabó, Z., and Bokor, J. (2014). Bridging the Gap between Theory and Practice in LPV Fault Detection for Flight Control Actuators. *Control Engineering Practice*, 31, 171–182.
- Varga, A. and Ossmann, D. (2014). LPV Model-based Robust Diagnosis of Flight Actuator Faults. *Control Engineering Practice*, 31, 135–147. doi: <https://doi.org/10.1016/j.conengprac.2013.11.004>.
- Wu, F. (1995). *Control of Linear Parameter Varying Systems*. Ph.D. thesis, University of California, Berkeley.
- Yamamoto, K., Koenig, D., Sename, O., and Moulairé, P. (2015). Driver Torque Estimation in Electric Power Steering System using an H_∞/H_2 Proportional Integral Observer. *2015 54th IEEE Conference on Decision and Control (CDC)*, 843–848.
- Yamamoto, K., Sename, O., Koenig, D., and Moulairé, P. (2019). Design and Experimentation of an LPV Extended State Feedback Control on Electric Power Steering Systems. *Control Engineering Practice*, 90, 123–132. doi: <https://doi.org/10.1016/j.conengprac.2019.06.004>.